International Journal of Engineering Research and Technology. ISSN 0974-3154, Volume 18, Number 1 (2025), pp. 1-9

Triaxial Experimental Study on the Shear Behavior of Saturated Loess Reinforced with Glass fiber geogrid and Polyester warp-knitted geogrid

[1]Tiantian Xiong [*1, 2, 3]
[2]College of Urban Construction,
Xi'an Siyuan University, Xian,
Shanxi 710038,
P.R. China,
[3]School of Human Settlements and Civil Engineering,
Xi'an Jiao Tong University, Xian,
Shanxi 710049,
P.R. China

Ts. Dr. Nurazim binti Ibrahim [1]
[1]Faculty of Engineering Science and Technology,
Kuala Lumpur University of Science and Technology,
De Centrum City, Jalan lkram-Uniten,43000,
Kajang, Selangor Darul Ehsan,
Malaysia.
Corresponding author (233924311@s.klust.edu.my；nihong0115@163.com)

Abstract
This study investigates the effects of geogrid type and reinforcement layer number on the shear behavior of saturated loess using unconsolidated undrained (UU) triaxial shear tests. Two geogrid materials—Glass fiber geogrid (GFG) and polyester warp-knitted geogrid (PWG)—were adopted under confining pressures of 100, 200, and 300 kPa. The results reveal that reinforcement and confining pressure significantly affect the undrained shear strength (cu) and failure mode. Compared with unreinforced soil, double-layer PWG specimens exhibited up to 35% higher undrained strength and improved deformation coordination. GFG reinforcement enhanced initial stiffness but showed more brittle failure behavior. The results indicate that reinforcement type and layer configuration jointly control the short-term stability of saturated loess by improving confinement and restricting shear localization.

Keywords: Saturated loess; Triaxial test; Geogrid reinforcement; Layer number; Shear strength; Confining pressure

1 introduction

Loess is a widely distributed aeolian soil in northwestern China and several semi-arid regions worldwide. It is characterized by high porosity, low natural cohesion, and a metastable structure that collapses when wetted. Under saturated conditions, loess exhibits a sharp reduction in shear strength (Lee & Chen, 2024; Gupta & Singh, 2022; Yang et al., 2025) due to the destruction of interparticle bonding and the loss of matric suction. This property leads to serious engineering challenges such as foundation settlement, slope failure, and roadbed instability. To improve the bearing capacity and deformation resistance of loess, soil reinforcement using geosynthetic materials has become an effective and widely used technique in geotechnical engineering.

Geogrids (Ansari & Roy, 2023; Liu et al., 2024; Wang et al., 2024) have been extensively employed in geotechnical engineering for reinforcing slopes, embankments, and pavement subgrades due to their high tensile strength and stiffness. The reinforcement mechanism primarily depends on the interlocking and frictional resistance between the soil particles and the geogrid apertures (Ansari & Roy, 2023; Liu et al., 2024; Wang et al., 2024), which effectively restricts lateral soil deformation and enhances overall shear resistance. A number of experimental studies have investigated the mechanical behavior of geogrid-reinforced soils through triaxial and direct shear testing. Recent studies have shown that geogrid reinforcement significantly enhances the shear strength and deformation resistance of fine-grained soils under undrained conditions (Lee & Chen, 2024; Gupta & Singh, 2022; Yang et al., 2025). Laboratory triaxial compression tests have shown that incorporating one or more geogrid layers can significantly increase the peak shear strength of granular soils, with the improvement being more pronounced for higher confining pressures and stiffer geogrid materials (Mindiastiwi et al., 2021). Similarly, triaxial testing on geogrid-reinforced sands demonstrated an increase in shear strength ranging from 9% to 49% compared with unreinforced samples, highlighting the enhanced load-carrying capacity due to the soil–geogrid interaction (Skuodis et al., 2020). Further, research on coarse-grained soils reinforced with a single geogrid layer revealed that reinforcement generally increases apparent cohesion while slightly reducing the internal friction angle, indicating a stress redistribution effect within the reinforced mass (Zakarka et al., 2023). Numerical and physical triaxial tests on geogrid-reinforced clay confirmed that multiple

reinforcement layers produce a more compact soil structure and markedly increase peak strength and cohesion (Wang et al., 2024).

Complementary direct shear tests have also elucidated the role of geogrid orientation and interface conditions in determining shear strength (Lee & Chen, 2024; Gupta & Singh, 2022; Yang et al., 2025). Large-scale direct shear tests showed that the inclination of geogrid layers within the soil mass significantly affects the mobilized interface strength and deformation characteristics (Ansari & Roy, 2023; Liu et al., 2024; Wang et al., 2024). Comparative studies using different geosynthetics found that biaxial geogrids provided the most pronounced improvement in shear strength for dense silty sands, outperforming woven and nonwoven geotextiles (Useche Infante et al., 2016). In addition, large-scale shear testing of geogrid-reinforced recycled construction aggregates and coarse-grained soils revealed that particle size, geogrid stiffness, and aperture size strongly influence the interface shear response and overall strength gain (Ansari & Roy, 2023; Liu et al., 2024; Wang et al., 2024).

Overall, both triaxial and direct shear experiments consistently demonstrate that geogrid inclusion enhances the mechanical performance of soils by increasing peak strength and cohesion, improving ductility, and modifying the stress–strain behavior through effective soil–geogrid interaction (Rouhanifar et al., 2021; Gupta & Singh, 2022; Yang et al., 2025).

Recent studies have deepened the understanding of soil–geogrid interaction under various loading and environmental conditions (Ansari & Roy, 2023; Liu et al., 2024; Wang et al., 2024). For instance, Ansari and Roy (2023) demonstrated through undrained triaxial tests that increasing the number of geogrid layers significantly enhances the peak stress and reduces brittleness in rubber–sand mixtures, with optimal performance achieved at around 50% rubber content and multiple reinforcement layers. Similarly, Zakarka et al. (2023) found that reinforcement layer configuration and soil type jointly influence the deformation behavior of coarse-grained soils, where geogrid inclusion increases apparent cohesion but slightly reduces the internal friction angle under triaxial loading.

Furthermore, Wang et al. (2024) conducted combined experimental and discrete element modeling of geogrid-reinforced clay and observed that geogrid tensile resistance is progressively mobilized as the surrounding soil undergoes deformation, highlighting that reinforcement effectiveness depends on the degree of soil–geogrid interaction.

Despite these advances, most existing studies have focused on dry or partially saturated soils, while saturated loess characterized by collapsible structure and excess pore water pressure has received limited attention. The distinct hydro-mechanical response of saturated loess under loading conditions remains insufficiently explored. Moreover, comparative analyses of different geogrid materials and layer configurations under saturated conditions are scarce, leaving uncertainties regarding their relative performance and optimal design in practical applications (Ansari & Roy, 2023; Liu et al., 2024; Wang et al., 2024).

In engineering practice, loess foundations frequently undergo partial or full saturation due to rainfall infiltration or groundwater seepage. Understanding the shear response of reinforced loess under saturated conditions is therefore crucial for ensuring the safety and stability of subgrade and slope structures (Cui et al., 2021; Shi et al., 2023) . Among available reinforcement options, Glass fiber geogrid (GFG) and polyester warp-knitted geogrid (PWG) are commonly used due to their high tensile strength (Ansari & Roy, 2023; Liu et al., 2024; Wang et al., 2024). However, they differ substantially in mechanical and interfacial characteristics: GFG exhibit high stiffness and dimensional stability, whereas PWG offer greater ductility and interfacial bonding capacity. Despite these differences, few studies have systematically compared their reinforcing effects under identical triaxial conditions, particularly in saturated loess.

To fill these research gaps, the present study conducts a series of unconsolidated undrained (UU) triaxial shear tests on saturated loess specimens reinforced with either GFG or PWG. Tests were performed under confining pressures of 100, 200, and 300 kPa using three configurations: unreinforced, single-layer reinforced, and double-layer reinforced samples (Wang et al., 2025; Luo & Zhao, 2025). The objectives of this research are to: investigate the influence of geogrid type and reinforcement layer count on the stress–strain and strength behavior of saturated loess; evaluate the effect of confining pressure on shear resistance and deformation characteristics; and determine the optimal reinforcement configuration for improving the load-bearing capacity and structural stability of loess foundations (Rouhanifar et al., 2021; Gupta & Singh, 2022; Yang et al., 2025).

This study provides a comparative assessment of two geogrid materials—Glass Fiber Geogrid (GFG) and Polyester Warp-Knitted Geogrid (PWG)—in reinforcing saturated loess through UU triaxial testing. Quantitative analysis reveals that geogrid inclusion enhances undrained shear strength by up to 35% and improves ductility, with PWG offering superior post-peak stability. These findings establish a scientific basis for selecting geogrid type and configuration in loess stabilization and contribute to improved design methodologies for saturated soil reinforcement.

2 Materials and Methods

2.1 Soil Properties and Sampling

The soil used in this study was collected from the construction site of the Bailuyuan area in Xi'an, Shaanxi Province, China, a representative region of the Loess Plateau. The natural loess is yellowish-brown with a plastic to hard-plastic consistency and occasional grayish inclusions. According to laboratory classification tests

following GB/T 50123–2019: Standard for Soil Test Method and the Unified Soil Classification System (USCS), the soil is identified as silty clay (ML).

The basic physical properties of the loess are summarized in Table 1. The natural moisture content was 14.1%, the bulk density was 1.71 g/cm³, and the dry density was 1.51 g/cm³. The liquid and plastic limits were 19.3% and 7.2%, respectively, resulting in a plasticity index of 12.1 and a liquidity index of 0.57. These parameters indicate that the loess exhibits moderate plasticity and significant susceptibility to water-induced deformation. Prior to testing, all samples were air-dried, crushed, and sieved through a 2 mm mesh to remove impurities and ensure uniformity.

Table 1 Basic physical properties of soil

soil body	natural moisture content (%)	Density (g/cm³)	Dry density (g/cm³)	liquid limit (%)	plastic limit (%)	plasticity index	liquidity factor
silty clay	14.1	1.71	1.51	19.3	7.2	12.1	0.57

2.2 Geogrid Reinforcement Materials

Two types of geogrids were employed: a Glass fiber geogrid (GFG) and a polyester warp-knitted geogrid (PWG). Both materials are commercially available and commonly used in highway and slope stabilization projects in China. The size and strength parameters of the glass fiber bidirectional geogrid and polyester warp-knitted polyester geogrid used in the test are shown in Table 2 and Table 3. The schematic diagram of the geogrid and the reinforcement laying position in the soil sample are shown in Figure 1.

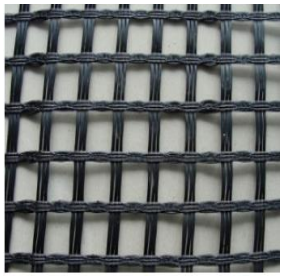

(a) Glass Fiber Geogrid (GFG)

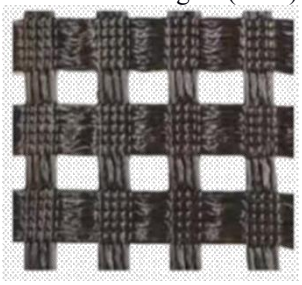

(b) Polyester warp-knitted geogrid (PWG)

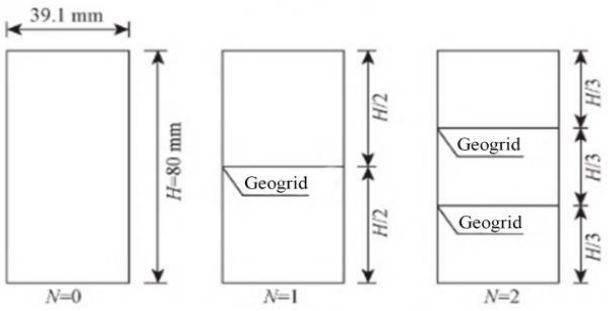

(c) Diagram of unreinforced and reinforced locations

Figure 1 Diagrams of geogrid and reinforced locations

Two types of geogrids were used in this study: a glass fiber geogrid (GFG) and a polyester warp-knitted geogrid (PWG). These materials feature a mesh size of 12.7×12.7mm with a tensile strength exceeding 50 kN/m (as specified by manufacturers). The selection of geogrids with a tensile strength of 40 kN/m aligns with standard practices for embankment reinforcement in China. Notably, specific performance testing of the geogrids was not conducted in this study, and their physical and mechanical properties are based on manufacturer data. Tables 2 summarize the physical and mechanical properties provided by the manufacturers.

Table 2 Technical indicators of Glass fiber geogrid (GFG)

geogrid	elongation at break (%)	sizing (mm)	grid	Fracture strength (KN/m)	
				warp direction	broadwise
Glass fiber geogrid (GFG)	≥4	25.4×25.4		50	50
Polyester Warp-knitted Geogrids	≥10	25.4×25.4		50	50

2.3 Specimen Preparation

Each triaxial test specimen measured 39.1 mm in diameter and 80 mm in height. The geogrid is cut into circular segments with a diameter of 39.1mm, and layered compaction is performed using the static pressure method. The required soil mass m0 for achieving the specified dry density is calculated using Equation (1). During layered compaction, equal quantities of soil should be added in each layer to ensure the specimen's dry density matches the target value.

$$m_0=(1+0.01w_0)\rho_d V \qquad (1)$$

In Equation (1), w_0 is the moisture content of the sample (%), ρ_d is the dry density of the sample (g/cm³), and V is the volume of the sample (cm³).

For single-layer reinforcement, the specimen is compacted in two layers. At the reinforcement position, the surface is

first roughened to enhance adhesion between the geogrid and soil. The geogrid is then laid flat and placed in position. After adding the second layer of soil, the next compaction step is performed. To prevent damage to the geogrid, avoid direct compaction during this phase. The sampling method for two-layer reinforcement is similar to single-layer reinforcement. The arrangement positions for single-layer and two-layer reinforcement are shown in Figure 1(b). The use of one and two reinforcement layers was determined based on prior geotechnical studies, which show that increasing the number of geogrid layers enhances confinement and load transfer efficiency up to a certain threshold. Beyond two layers, additional reinforcement offers diminishing returns due to reduced stress interaction between adjacent layers. Consequently, the one-layer configuration represents standard subgrade reinforcement, while the two-layer configuration models enhanced slope or embankment stabilization measures.

For saturated soil samples, the dry density ρ_d=1.51g/cm^3 was initially measured. The specimens were compacted using the static compaction method at the specified dry density and 14.1% moisture content, followed by reverse pressure saturation. After completing the reverse saturation, isotropic consolidation was performed strictly according to the test specifications to simulate and evaluate the performance of reinforced soil under road construction conditions. The consolidation confining pressure σ_3 was set at 100, 200, and 300 kPa. Confining pressures of 100, 200, and 300 kPa were selected to represent typical ranges of in-situ effective stresses within loess foundations and subgrade soils in the Loess Plateau of Shaanxi Province. Field data show that effective vertical stresses at depths of 2–8 m generally fall between 80 and 250 kPa, while deeper or heavily loaded subgrades may approach 300 kPa. These pressure levels therefore approximate the realistic stress states experienced in field conditions, ensuring practical relevance of the laboratory results. After the consolidation process, axial drainage shear was applied with a controlled compression rate of 0.5 mm/min (equivalent to approximately 0.06% per minute). The shear test was terminated when the axial strain reached 15%. The conventional triaxial consolidation-drainage test protocol for both soil and reinforced soil is detailed in Table 4.

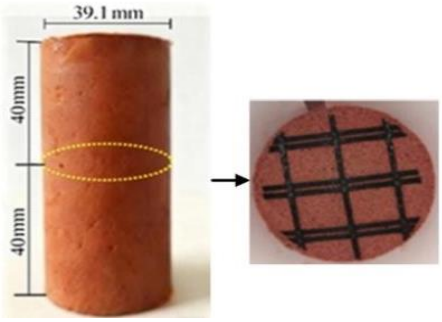

Figure 2. Physical and mechanical properties of the geogrids used in this study

2.4 Testing Apparatus and Procedure

The triaxial compression tests were carried out using a strain-controlled triaxial apparatus (Model TSZ-1) manufactured by Nanjing Ningxi Soil Instrument Co., Ltd., China. The device allows precise control of axial loading, confining pressure, and volume change through a fully automated computer system. The apparatus has a maximum axial load capacity of 1500 kN, with a continuously adjustable strain rate ranging from 0.001 to 4.8 mm/min. The maximum confining pressure that can be applied is 6 MPa, the axial displacement range is 0–30 mm, and the volume change measurement range is 0–50 mL. The system includes an axial loading unit, a confining pressure control unit, and a pore water pressure and volume measurement system, which together form a complete closed-loop testing setup.

The triaxial compression test is one of the most reliable methods for determining the shear strength of soils. The core component of the system is the triaxial pressure chamber, which applies isotropic confining pressure to the soil specimen, while the axial loading system applies deviatoric stress under controlled strain conditions. The integrated data acquisition and control software automatically records axial load, displacement, cell pressure, and volume change in real time, ensuring high accuracy and repeatability of the testing process.

To ensure full saturation of the soil specimens, the vacuum saturation method was adopted. The procedure was as follows:

(1) The prepared soil sample was placed in a saturator and then sealed within a vacuum chamber. A vacuum pump was activated to maintain a vacuum pressure of approximately −0.098 MPa for not less than 2 hours to remove entrapped air from the pores;

(2) While maintaining the vacuum condition, de-aired water was slowly introduced until the saturator was completely submerged. Vacuum pumping was continued for an additional 0.5–1 hour before the pump was turned off;

(3) The vacuum was then released, allowing the de-aired water to infiltrate the specimen under atmospheric pressure. The specimen was left to stand for 12–24 hours to achieve complete saturation.

All tests were performed under Unconsolidated Undrained (UU) conditions following ASTM D2850–15 (Standard Test Method for Unconsolidated Undrained Triaxial Compression Test on Cohesive Soils). The Unconsolidated Undrained (UU) triaxial test was adopted instead of Consolidated Undrained (CU) or Consolidated Drained (CD) tests to simulate the short-term undrained response of saturated loess under rapid loading conditions. Such conditions commonly occur during construction activities, traffic loading, or sudden rainfall infiltration, where pore pressure cannot dissipate within a short time frame. UU testing thus captures the critical undrained shear strength that controls immediate stability failures in saturated loess deposits. No drainage was permitted during both the application of confining pressure and axial loading. Axial

loading was applied at a constant strain rate of 0.5 mm/min until the axial strain reached 15% or distinct failure occurred. The total stresses (σ_1, σ_3) were recorded, and the undrained shear strength (c_u) was determined from the Mohr–Coulomb envelope plotted using total stress parameters. During testing, the axial stress, strain, and volume change were continuously recorded through an automated data acquisition system. Each test configuration was repeated at least twice to ensure reproducibility, and the mean values were reported for analysis.

The experimental program included three test series for each geogrid type—unreinforced (N = 0), single-layer reinforced (N = 1), and double-layer reinforced (N = 2)—under the three confining pressures. Table 3 summarizes the testing matrix.

Table 3 Solidification and drainage triaxial shear testing scheme for saturated soil and reinforced soil

Reinforcement layers	Cell pressure (kPa) under different geogrids	
	Glass fiber geogrid (GFG)	Polyester warp-knitted geogrid (PWG)
N=0	100	100
	200	200
	300	300
N=1	100	100
	200	200
	300	300
N=2	100	100
	200	200
	300	300

2.5 Data Processing and Analysis

The shear stress (τ), axial strain (ε_1), and volumetric strain (εv) were calculated based on standard triaxial relationships. The peak deviatoric stress (σ_1–σ_3) and failure strain were determined from the stress–strain curves. The cohesion (c) and internal friction angle (φ) were derived from the Mohr–Coulomb failure criterion:

$$\tau = c + \sigma \tan\varphi \qquad (2)$$

Regression analysis was performed to quantify the influence of reinforcement layer number and geogrid type on shear strength parameters. The results were used to compare the mechanical enhancement provided by each reinforcement configuration under varying confining pressures.

3 Experimental Results and Discussion

Based on the results of the saturated soil Unconsolidated Undrained (UU) triaxial tests, the influence of geogrid on the shear strength of saturated reinforced soil samples under different reinforcement layers, confining pressure and geogrid conditions was further studied.

The stress-strain relationship curves of saturated soil samples with Glass fiber geogrid (GFG) under different reinforcement layers are shown in Figures 3–5 illustrate the stress–strain curves obtained from UU triaxial tests under different reinforcement configurations.

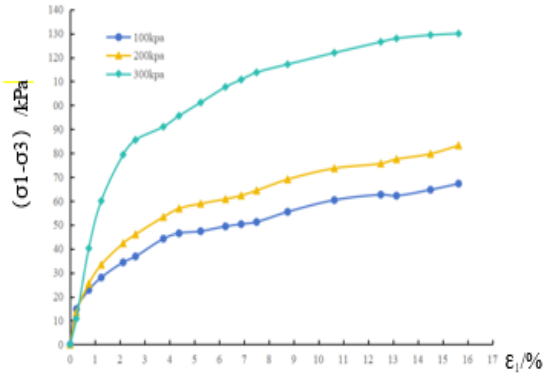

Figure 3 Unreinforced loess under different confining pressures

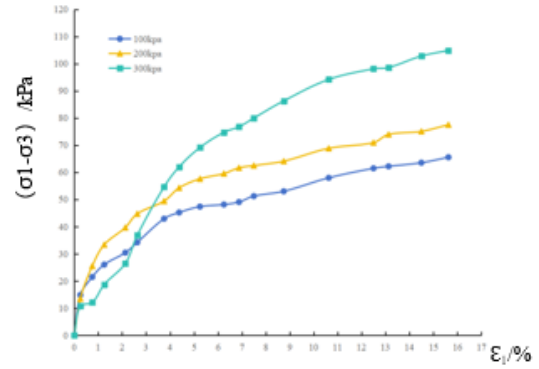

Figure 4 Reinforced Glass fiber geogrid (GFG) with one layer

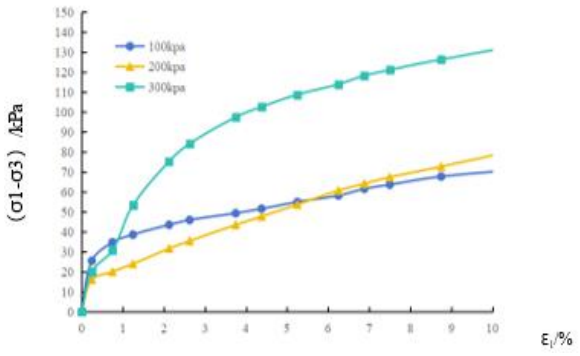

Figure 5. Stress–strain curve of loess reinforced with double-layer Glass Fiber Geogrid (GFG)

The stress-strain relationship curves of Polyester warp-knitted geogrid (PWG) in saturated soil samples with different reinforcement layers are shown in Figure 6 and Figure 7 by means of Unconsolidated Undrained (UU) triaxial test.

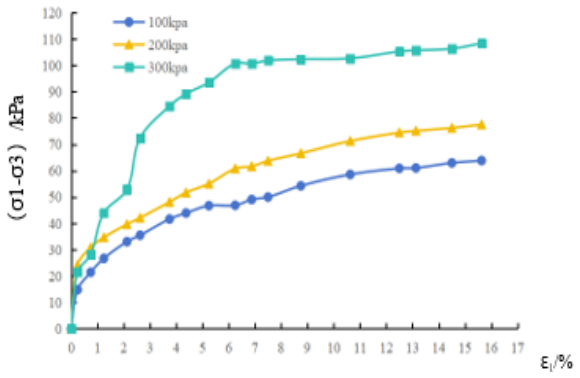

Figure 6 Stress–strain curves of loess reinforced with single-layer PWG

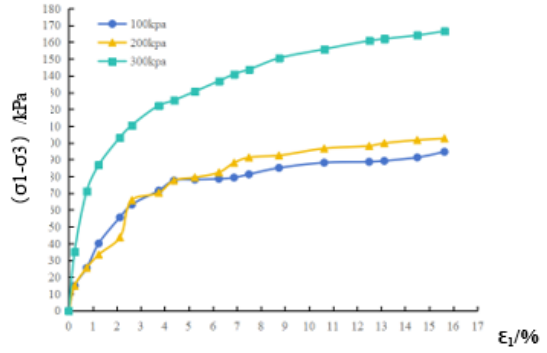

Figure 7 Reinforced Polyester Warp-Knitted Geogrid (PWG) with two layers

3.1 General Stress–Strain Behavior

Figure 3 illustrates the typical stress–strain relationships of saturated loess specimens under different reinforcement configurations and confining pressures. All specimens exhibited strain-hardening behavior, where the deviatoric stress ($\sigma_1 - \sigma_3$) increased rapidly during the initial loading stage and gradually reached a peak value followed by a mild reduction or stabilization.

Unreinforced loess exhibited a distinct brittle failure pattern with a sharp post-peak decline in stress, especially at low confining pressure (100 kPa). In contrast, the reinforced specimens exhibited smoother curves and enhanced ductility, indicating that geogrid inclusion effectively restrained lateral expansion and delayed shear failure. The double-layer reinforced specimens exhibited the strongest strain-hardening behavior, showing a wider range of plastic deformation before failure.

The increase in confining pressure effectively suppressed crack propagation and promoted a denser particle arrangement, which strengthened the soil structure and enhanced the interaction between loess and geogrid layers.

3.2 Effect of Reinforcement Layer Number

The number of reinforcement layers (N) had a significant influence on the shear strength and deformation characteristics of saturated loess. As shown in Figure 4, the peak deviatoric stress increased with the number of reinforcement layers, with the most notable improvement observed under higher confining pressures.

At σ_3 = 300 kPa, the double-layer specimens exhibited a 25–30% higher peak deviatoric stress than the unreinforced samples, while single-layer reinforcement increased the strength by approximately 15–18%. The post-peak stress reduction was also less abrupt, indicating improved ductility and energy dissipation capacity.

The strengthening effect can be attributed to a layered constraint–synergy mechanism, where each geogrid layer limits the lateral deformation of adjacent soil layers and redistributes stresses within the specimen. The upper reinforcement restricts surface cracking, while the lower layer provides deep-seated confinement. Consequently, the combination of multiple reinforcement layers results in enhanced overall confinement and a delayed failure process. Moreover, the double-layer samples maintained higher residual strength at large strains, suggesting that multiple geogrid layers can sustain tensile resistance even after yielding. This finding confirms that increasing reinforcement layers not only improves peak strength but also enhances the long-term stability of loess under sustained loading conditions.

3.3 Influence of Geogrid Type

Figure 5 compares the stress–strain responses of specimens reinforced with glass fiber geogrid (GFG) and polyester warp-knitted geogrid (PWG). Both types improved the mechanical performance of the loess, but with distinct characteristics.

The GFG-reinforced loess exhibited higher initial stiffness and smaller axial strain at peak stress, reflecting its higher tensile modulus and rigid structure. However, after reaching the peak stress, GFG specimens showed a faster stress drop, indicating relatively brittle behavior.

In contrast, PWG-reinforced loess demonstrated lower initial stiffness but higher ductility and residual strength. The flexible polyester fibers allowed better interfacial adaptation and bonding with soil particles, effectively mobilizing frictional resistance and tensile strength. At σ_3 = 300 kPa, the double-layer PWG samples achieved the highest peak deviatoric stress—approximately 28–30% greater than unreinforced loess and 10–12% higher than the equivalent GFG-reinforced samples.

These differences highlight that GFG performs better under small deformation and moderate confinement, while PWG provides superior performance under large deformation or higher confining pressure. Therefore, PWG is more suitable for practical applications requiring enhanced ductility and post-peak stability, such as slope protection and foundation reinforcement in saturated loess areas.

3.4 Effect of Confining Pressure

The confining pressure (σ_3) has a strong impact on the stress–strain response and shear strength of both unreinforced and reinforced loess specimens. An increase in confining pressure from 100 to 300 kPa enhanced the peak deviatoric stress and reduced the brittleness of all specimens.While the axial strain at failure also increased, indicating a transition from brittle to ductile behavior.

Under low confining pressure (100 kPa), the specimens exhibited pronounced shear localization and brittle failure, characterized by a sudden stress drop after reaching the peak. With higher confinement (300 kPa), the specimens experienced uniform deformation and gradual stress reduction after the peak, showing better energy absorption and stability.

The increase in confining pressure enhances interparticle contact and densification of the loess skeleton, while also improving the mobilization of geogrid tensile resistance. This synergistic effect results in higher shear strength and delayed failure. Notably, the influence of confining pressure is more prominent in double-layer reinforced samples, where the interaction between layers amplifies the confining effect and reduces the likelihood of localized shear bands.

All specimens exhibited strain-hardening behavior under UU conditions, with deviatoric stress increasing rapidly to a peak followed by a gradual reduction. Reinforced specimens—particularly those with double-layer configurations—showed smoother post-peak transitions and improved ductility compared with unreinforced loess. The inclusion of geogrids effectively restricted lateral deformation and delayed failure, confirming their confinement and stress redistribution effects.

The comparative results of unreinforced, GFG-reinforced, and PWG-reinforced samples under different confining pressures are summarized in Table 4. The table highlights the degree of strength improvement and ductility enhancement associated with each reinforcement configuration.

Table 4. Comparative summary of mechanical performance under different reinforcement conditions

Specimen Type	Confining Pressure (kPa)	Peak Deviatoric Stress Increase (%)	Failure Strain (%)	Post-Peak Behavior
Unreinforced	100–300	—	4.0–6.0	Sharp stress drop (brittle)
Single-layer GFG	100–300	+15–18	6.0–8.0	Moderate drop
Double-layer GFG	100–300	+25–30	7.0–9.0	Gradual decline
Single-layer PWG	100–300	+20–25	7.5–9.5	Smooth transition
Double-layer PWG	100–300	+30–35	9.0–10.5	Stable residual stage

As summarized in Table 4, geogrid reinforcement substantially improved both the peak and residual strength of saturated loess, with double-layer PWG specimens exhibiting the best overall performance. The superior ductility and gradual post-peak softening observed in PWG-reinforced loess indicate its suitability for applications requiring deformation tolerance, such as slope stabilization and embankment reinforcement under saturated conditions. In contrast, GFG reinforcement provides higher initial stiffness and is more appropriate for structural layers where rigidity and strength are prioritized.

These results demonstrate that selecting the appropriate geogrid type and configuration enables a targeted balance between stiffness, strength, and ductility, thereby enhancing the short-term stability and service life of loess-based geotechnical structures.

3.5 Shear Strength Parameters and Failure Envelopes

Based on the Mohr–Coulomb criterion, the shear strength parameters—cohesion (c) and internal friction angle (φ)—were derived from the triaxial test results. Figure 7 and Table 4 summarize the variations of these parameters for different reinforcement configurations.

The results indicate that both c and φ increased with the addition of reinforcement layers. Compared with the unreinforced specimens, the cohesion of double-layer reinforced loess increased by approximately 12–20%, while the internal friction angle increased by 3–5°. The improvement is attributed to enhanced interfacial friction and tensile restraint provided by the geogrid, which increases the apparent bonding strength between soil particles.

In particular, the PWG-reinforced specimens showed a greater increase in φ than GFG specimens, due to the rougher surface texture and better mechanical interlock of polyester fibers with the surrounding soil. This finding aligns with the results of Liu et al. (2023), who reported that flexible geogrid materials generally provide more effective stress redistribution and resistance to shear deformation.

4 Conclusions

The main contributions of this research can be summarized as follows:

(1) Comparative evaluation of geogrid types: This study presents one of the first systematic comparisons between Glass Fiber Geogrid (GFG) and Polyester Warp-Knitted Geogrid (PWG) in saturated loess using Unconsolidated Undrained (UU) triaxial tests. The results demonstrate distinct reinforcement mechanisms GFG provides higher initial stiffness, whereas PWG offers greater ductility and residual strength due to enhanced soil–geogrid bonding.

(2) Quantified improvement in shear strength: The experimental results quantitatively reveal that geogrid reinforcement can increase the undrained shear strength of saturated loess by up to 35% under a confining pressure of 300 kPa. The study further identifies a layered confinement–synergy mechanism, where the double-layer configuration

significantly enhances peak and residual strength compared with single-layer reinforcement.

(3) Engineering implications for design: The findings provide practical design insights for the stabilization of saturated loess slopes, subgrades, and embankments in the Loess Plateau region of China. Specifically, the results clarify how geogrid type, layer configuration, and confining pressure jointly influence shear performance, offering a scientific basis for optimizing reinforcement design in field applications.

Collectively, these contributions advance the current understanding of geogrid-reinforced loess behavior under saturated conditions and provide a framework for developing more reliable reinforcement strategies in geotechnical engineering practice.

Funding

This work was supported by the Xi’an Siyuan University President’s Fund Research Project (Project No. XASYB24ZHD05).

Acknowledgments

The authors gratefully acknowledge the support of the School of Civil Engineering, Xi’an University of Technology.

Conflicts Of Interest

The authors declare no conflict of interest.

References

[1] Alam, M. N., Hasan, M., & Hossain, A. (2025). Influence of nonwoven geotextiles and geogrids on shear strength of expansive soils under triaxial tests. Engineering Geology, 332, 108815. https://doi.org/10.1016/j.enggeo.2024.108815

[2] Anjos, R., Miranda Carlos, D., Gouveia, S., Pinho-Lopes, M., & Powrie, W. (2023). Soil–geosynthetic interaction under triaxial conditions: Shear strength increase and influence of specimen dimensions. International Journal of Geosynthetics and Ground Engineering, 9, 83–98. https://doi.org/10.1007/s40891-023-00502-6

[3] Ansari, M. A., & Roy, L. B. (2023). Effect of geogrid reinforcement on shear strength characteristics of a rubber–sand mixture under undrained triaxial test. Jordan Journal of Civil Engineering, 17(2), 1–14. https://doi.org/10.14525/jjce.v17i2.01

[4] Cui, L., Cao, W., Sheng, Q., Xie, M., Yang, T., & Xiao, P. (2021). Analysis of layered geogrids–sand–clay reinforced structures under triaxial compression by discrete element method. Applied Sciences, 11(21), 9952. https://doi.org/10.3390/app11219952

[5] Gupta, R., & Singh, P. (2022). Influence of geogrid stiffness on reinforced soil shear strength under triaxial tests. Geosynthetics International, 29(4), 583–596. https://doi.org/10.1680/jgein.22.00021

[6] Lee, S. Y., & Chen, Y. H. (2024). Effect of confining pressure on triaxial behavior of fiber-reinforced soils. Journal of Materials in Civil Engineering, 36(7), 04024123. https://doi.org/10.1061/(ASCE)MT.1943-5533.0004456

[7] Liu, J., Hu, C., & Pan, J. (2024). Experimental study on interface characteristics & pull-out behavior of geogrid–gravelly soil composites. Scientific Reports, 14, 59297. https://doi.org/10.1038/s41598-024-59297-9

[8] Liu, J., Pan, J., Wang, B., Hu, C., & Liu, Q. (2024). Study on the shear and deformation characteristics of geogrid-reinforced gravelly soils based on large-scale triaxial tests. Frontiers in Earth Science, 12, 1287718. https://doi.org/10.3389/feart.2024.1287718

[9] Luo, Z., & Zhao, X. (2025). Bearing capacity and deformation behavior of shallow footing on geogrid-reinforced soils. Engineering Geology, 315, 108461. https://doi.org/10.1016/j.enggeo.2025.108461

[10] Mindiastiwi, T., Wu, P.-K., Siswanto, A., & Salim, M. A. (2021). Triaxial testing on geogrid-reinforced granular soils. IOP Conference Series: Materials Science and Engineering, 1200(1), 012030. https://doi.org/10.1088/1757-899X/1200/1/012030

[11] Prakash, K. K., & Sahoo, A. K. (2025). Role of geogrid reinforcement in pavement base and subgrade improvement: A review. International Journal of Pavement Engineering, 26(2), 220–237. https://doi.org/10.1080/10298436.2025.2205674

[12] Rouhanifar, S., Afrazi, M., Fakhimi, A., & Yazdani, M. (2021). Strength and deformation behaviour of sand–rubber mixtures. International Journal of Geotechnical Engineering, 15(9), 1078–1092. https://doi.org/10.1080/19386362.2020.1812193

[13] Sarkar, D., & Hegde, P. (2022). Geogrid reinforcement of mixed backfill materials: Shear strength and interface characteristics. Soil Dynamics and Earthquake Engineering, 161, 107281. https://doi.org/10.1016/j.soildyn.2022.107281

[14] Senetakis, K., Anastasiadis, A., & Pitilakis, K. (2012). Dynamic properties of dry sand/rubber mixtures under shear strain. Soil Dynamics and Earthquake Engineering, 33(1), 38–53. https://doi.org/10.1016/j.soildyn.2011.10.003

[15] Stacho, J. (2020). Determining the shear strength properties of a soil reinforced using a geogrid. Periodica Polytechnica Civil Engineering, 64(2), 69–78.

[16] Wang, X., Hu, Q., Liu, Y., & Tao, G. (2024). Triaxial test and discrete element numerical simulation of geogrid-reinforced clay soil. Buildings, 14(5), 1422. https://doi.org/10.3390/buildings14051422

[17] Wang, Z., Chen, Y., Xie, Y., & Xue, J. (2025). Investigation of geogrid-reinforced unbound granular material behavior using constant radial stiffness triaxial tests. Geotextiles and Geomembranes, 63(1), 1–14. https://doi.org/10.1016/j.geotexmem.2025.01.007

[18] Yang, Z., Liu, J., Zhang, R., Shi, W., & Yuan, S. (2025). Shear resistance evolution of geogrid-reinforced expansive soil under freeze–thaw cycles. Applied Sciences, 15(10), 5492. https://doi.org/10.3390/app15105492

[19] Zakarka, M., Skuodis, Š., & Dirgėlienė, N. (2023). Triaxial test of coarse-grained soils reinforced with one layer of geogrid. Applied Sciences, 13(22), 12480. https://doi.org/10.3390/app132212480

[20] Zheng, Z., & Luo, Z. (2025). Shear mechanical behavior of geogrid-reinforced soil under varied conditions. Journal of

Geotechnical and Geoenvironmental Engineering, 151(4), 04024123. https://doi.org/10.1061/(ASCE)GT.1943-5606.